Article

Limnospira indica PCC8005 and *Lacticaseibacillus rhamnosus* GG Mixed Dietary Combination Reduces Pelvic Irradiation-Induced Symptoms in Mice

Sarah-Renée Gholam [1,2], **Charlotte Segers** [1], **Mohamed Mysara** [1,†], **Amelie Coolkens** [1], **Sarah Baatout** [1], **Natalie Leys** [1] and **Felice Mastroleo** [1,*]

1   Nuclear Medical Applications, Belgian Nuclear Research Centre, SCK CEN, 2400 Mol, Belgium; sarah-renee.gholam@vub.be (S.-R.G.); charlotte.segers@sckcen.be (C.S.); mmaysara@nu.edu.eg (M.M.); sarah.baatout@sckcen.be (S.B.); natalie.leys@sckcen.be (N.L.)
2   VIB-VUB Center of Structural Biology, 1040 Brussels, Belgium
*   Correspondence: felice.mastroleo@sckcen.be
†   Current address: Bioinformatics Group, Center of Informatics Science, Nile University, Giza 41516, Egypt.

Abstract: Throughout their cancer treatments, around half of all patients will undergo irradiation that is accompanied by several side effects reducing their quality of life and leading to the interruption or extension of their treatment course. Pelvic irradiation leads to the triggering of mucositis and dysbiosis, further impairing the daily life of the patients. In this work, we address the ability of *Limnospira indica* strain PCC 8005 and *Lacticaseibacillus rhamnosus* GG ATCC 53103 in alleviating the above-mentioned side effects triggered by the local pelvic irradiation of 12 Gy in a mouse model. We found that the combinatorial administration of these food supplements was able to confer partial tight junction protection while the bacterial translocation towards the mesenteric lymph nodes was found to be identical between the saline sham-irradiated and supplemented irradiated group. Furthermore, the supplemented group did not present a significant shift in microbial composition following pelvic irradiation, indicating that the bacterial formulation was able to mitigate the dysbiosis induced by the latter treatment, as observed in the saline irradiated group. These very promising results will be further completed by investigating the mode of action and/or active molecules mediating the beneficial effects of both *L. indica* PCC 8005 and *L. rhamnosus* GG.

Keywords: gut microbiota; microbiome; pelvic irradiation; *Limnospira indica*; *Lacticaseibacillus rhamnosus* GG; natural food supplement; mouse radiotherapy model

1. Introduction

As the human lifespan increases, more and more diseases are being discovered and treatments investigated to improve the quality of life of the aging population. Cancer has become the leading cause of death in 57 countries [1]. In 2020, around 19.3 million new cancer cases were recorded worldwide, with almost 10 million cancer deaths, 9.4% of which were due to colorectal cancer, 8.3% [2]. The number of new cancer cases is expected to increase by 47% in 2040, excluding the possible increase in smoking, obesity, or unhealthy diets [2]. Furthermore, new environmental factors have emerged, such as increasing pollutants containing carcinogens that can be found in food, air, or water.

Several treatments are available and administered to patients according to their cancer stage (I–II–III–IV). For instance, chemotherapy and radiotherapy are administered to rectum stage IV cancer patients, exclusively, with a 12% survival rate [3]. Importantly, cancer treatments frequently present off-target effects. Thus, 80% of rectal cancer patients that undergo radiotherapy experience moderate to severe incontinence in their course of treatment [4], and as much as 22% of patients that received pelvic radiotherapy expressed an impairment in their social function due to irritated bowels within three months following

therapy [5]. The gastrointestinal mucositis observed following irradiation can be defined as the inflammation and/or ulceration of the oral and/or gastrointestinal tract, originating from medication, irradiation, or infectious diseases for instance [1]. The pathology induced by pelvic irradiation is first characterized by an acute phase defined by diarrhea, nausea, abdominal pain, and incontinence, developing during the first 2 to 3 weeks of treatment. Then, chronic bowel toxicity presents itself 6 months to 3 years following treatment and is characterized by altered transit, dysmotility, and intestinal perforation [2,3]. These various undesired effects following pelvic irradiation can be attributed to the exposure of the surrounding healthy tissues to ionizing radiation. This can then lead to inflammation, epithelial barrier impairment, and dysbiosis. The latter is defined as an imbalance in a microbial population such as the gut microbiota. Dysbiosis can be associated with diseases such as obesity and inflammatory bowel disease [4].

To improve the quality of life of radiotherapy patients, different compounds have been investigated for their radioprotective properties. *Lacticaseibacillus rhamnosus* GG and *Limnospira indica* PCC 8005 are being studied at SCK CEN as potential microbial therapies to confer beneficial properties to the host when administered in an adequate amount. *L. rhamnosus* GG is a Gram-positive bacterium found in various yogurts as a probiotic agent, proposed to positively impact the intestinal microbial population of the host. Furthermore, *L. rhamnosus* GG supplementation in healthy female mice was proven to influence the microbial gut population by promoting the abundance and diversity of the microbial population. Indeed, at the phylum level, the number of *Bacteroidetes* members, a member of the commensal intestinal flora, increased while the *Proteobacteria* population decreased [5]. At the genus level, *Eubacterium nodatum*, *Prevotellaceae* UCG, and *Parabacteroides*, for instance, were found to be more abundant in the group receiving *L. rhamnosus* GG. *L. indica* PCC8005, also known as *Spirulina*, have been consumed by humans for centuries and have recently been shown to exhibit unique radioresistant properties in vitro [6]. Recently, Segers et al. were also able to demonstrate the ability of *L. indica* PCC 8005 supplementation and *L. rhamnosus* GG supplementation in preventing the dysbiosis induced by pelvic irradiation in a mouse model [7]. Furthermore, when the latter was administered to mice as living cells, an increase was observed in the abundance of *Lachnospiraceae* and *Porphyromonadaceae* members, known for producing healthy gut barrier enhancer butyrate [8].

As a follow-up study and to assess the potential synergetic effect of combined supplementation, we fed our mouse model for pelvic irradiation with both *L. indica* PCC 8005 and *L. rhamnosus* GG living cells, ultimately attempting to improve the quality of life of radiotherapy patients.

2. Materials and Methods

2.1. Mice

Five-week-old male mice C57BI/6JRj were purchased from Janvier (Bio Services, Uden, The Netherlands) and housed individually, in ventilated cages under standard laboratory conditions, 12 h of light/dark cycles. Access to water and regular chow was provided *ad libitum*. Upon arrival, they were weighted and acclimatized for two weeks before the beginning of the experiments. To avoid confounding factors (e.g., hormones), only male mice were used. In addition, they were randomly assigned to a group using the *minDiff* package in RStudio (v.2021.09.0, Posit RStudio, Boston, MA, USA).

The mice were housed in compliance with the Ethical Committee Animal Studies of Medanex Clinic (EC MxCl 2018-093). The entirety of the animal experiments was conducted in accordance with the Belgian laboratory animal legislation and the European Communities Council Directive of 22 September 2010 (2010/63/EU).

2.2. Bacterial Strains and Growth Conditions

In this experiment, the P1 strain of *Limnospira indica* PCC 8005 was used. P1 is formed of helical trichromes, originally obtained from the Pasteur Collection of Cyanobacteria (PCC) (Institut Pasteur, Paris, France). *L. indica* PCC 8005 was grown axenically in 250 mL

Erlenmeyer's in 95 mL of modified Zarrouk medium [9], at a pH of around 9.8, at a constant temperature of 30 °C in a Binder incubator (Analis SA, Suarlée Belgium), at 100 rpm on an Edmund Bühler KS-15 rotary shaker (Edmund Bühler, Bodelshausen, Germany). The cyanobacteria were illuminated with a photon flux density of 50 μmol photons $\times$ m^{-2} $\times$ s^{-1} produced by Osram Daylight tubes (Osram, Zellik, Belgium). Sterile conditions were assessed using axenicity tests in 50 mL tissue culture flasks consisting of 9 mL of Luria Bertani (LB) broth and 1 mL of *L. indica* PCC 8005 culture, and in parallel, 8 mL of LB broth, 1 mL of Zarrouk medium and 1 mL of *L. indica* PCC 8005 exposed to the same conditions as previously mentioned.

To prepare fresh bacterial biomass for supplementation, *L. indica* PCC 8005 was grown for 14 days to reach the mid-log phase corresponding to OD$_{750}$ $\approx$ 1 using a Nanocolor UV/VIS spectrophotometer (Macherey-Nagel, Duren, Germany). *L. indica* PCC 8005 was centrifuged the first time at 10,000$\times$ *g* for 10 min at room temperature, then washed 3 times with sterile saline. Finally, the pellet was resuspended in 2700 μL of sterile saline to reach the desired bacterial concentration per 200 μL administered to the mice by oral gavage, as previously performed [8].

Simultaneously, *L. rhamnosus* GG ATCC 53103 was obtained from the University of Antwerp (Antwerp, Belgium), from the laboratory of Sarah Lebeer. *L. rhamnosus* GG was grown in 10 mL of de Man, Rogosa, and Sharpe (MRS) (BD, Olen, Belgium) medium at a constant temperature of 37 °C, in the dark, in static conditions in a Binder BC53 incubator (Analis SA, Suarlée Belgium). The mid-log phase was reached after approximately 10 h, OD$_{600}$ $\approx$ 0.25 using a BioPhotometer (Eppendorf, Aarschot, Belgium). The fresh biomass for oral administration to the mice was prepared by first centrifuging at 10,000$\times$ *g* for 5 min at 4 °C, followed by three washing steps using sterile saline, to finally resuspend the pellet in 3 mL of sterile saline to reach the desired bacterial concentration per 200 μL for administration.

2.3. Experimental Setup

The first experimental batch of mice received was randomly divided into three groups and treated for two weeks according to the following setup: a first group of mice (*n* = 10) receiving saline (200 μL/mouse$\times$day) and a pelvic irradiation dose of 0 Gy (i.e., sham-irradiated), a second group (*n* = 10) receiving saline (200 μL/mouse$\times$day) and a pelvic irradiation dose of 12 Gy, and finally a third group (*n* = 9) receiving the food supplement and a 12 Gy irradiation of the pelvic region (Figure 1). The food supplementation of the first group consisted of a daily alternation between *L. rhamnosus* GG and *L. indica* PCC 8005 at ~7 $\times$ 10^8 cells/mouse$\times$day and ~3 $\times$ 10^7 cells/mouse $\times$ day, respectively, administered by oral gavage. The second experimental batch of mice was also randomized into 3 different groups, following the above-mentioned setup, and treated for three weeks.
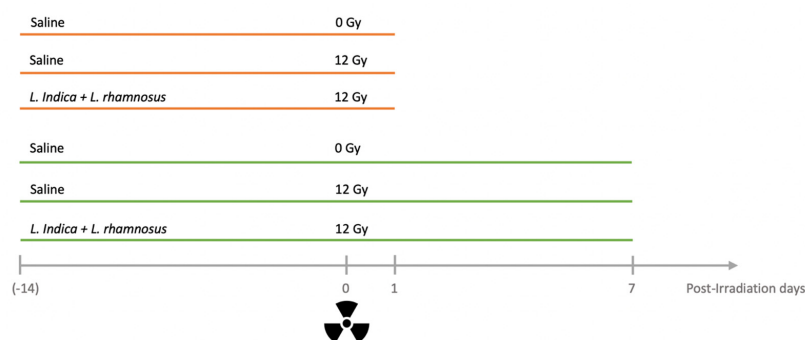

Figure 1. Experimental setup of supplemented and non-supplemented mice. Two time points were studied, PID1 (orange) and PID7 (green), corresponding to the day of sacrifice following pelvic irradiation. For each time point, three groups of mice were used: Saline 0 Gy (*n* = 10), Saline 12 Gy (*n* = 10) and Supplemented 12 Gy (*n* = 9). PID = post-irradiation day.

Each day during the experimental setup, mice were weighed, and feces were collected for the second batch only. Following the supplementation time of 15 days, mice were (sham-) irradiated and sacrificed at post-irradiation day (PID) 1 for the first experimental batch and at PID7 for the second experimental batch. The supplementation was carried out until the day of sacrifice.

2.4. Irradiation Protocol and Sacrifice

Following 14 days of bacterial supplementation, nine weeks-old mice were anesthetized using 50 mg/kg of ketamine hydrochloride (Nimatek, Eurovet Animal Health, Bladel, The Netherlands) and 0.25 mg/kg of medetomidine hydrochloride (Domitor, Orion Corporation, Espoo, Finland) by intraperitoneal injection as previously performed [3]. To avoid blindness caused by dried-out eyes, a gel composed of 2 mg/kg of carbomerum (Vidisic, Bausch + Lomb, Schaerbeek, Belgium) was applied. Once anesthetized, a maximum of 7 mice were placed and taped in a custom-made Plexiglas box (20 cm diameter and 5 cm height) allowing the right positioning of the pelvic area towards the center using a lead shield exposing exclusively the pelvic area in a 9 cm diameter circle [3]. The transportation to the irradiation facility was performed using a HEPA filter bag to ensure sterility. Heating plates (Pavan Service, Oud-Turnhout, Belgium) were also used to maintain the body temperature between 35 and 37 °C during the entire procedure.

A single dose of 12 Gy X-irradiation was administered using an Xstrahl 320 kV tube at a dose rate of 0.78 Gy/min in a vertical orientation, in accordance with ISO 4037 and under ISO 17025 accreditation, as previously performed [3]. Again, the body temperature of the mice was maintained between 35 and 37 °C by placing the box on a heating plate. The control mice not receiving irradiation were also anesthetized and kept under anesthesia for the same amount of time to rule out any confounding effect. The anesthesia was then reversed using atipamezole hydrochloride (Antisedan, Orion Corporation, Espoo, Finland) at a concentration of 1 mg/kg via intraperitoneal injection. The mice were placed in a heating chamber to again maintain body temperature during waking up. Following the irradiation protocol, the first group of mice was sacrificed at PID1, while the second group was sacrificed at PID7.

2.5. Bacterial Translocation to the Mesenteric Lymph Nodes

The mesenteric lymph nodes collected aseptically and stored in sterile saline were first homogenized 5 times using a 40 µm nylon cell strainer (VWR, Leuven, Belgium) and a 10 mL syringe plunger. The homogenized cell suspension was then diluted 1:10 in filtered phosphate-buffered saline. This volume was again filtered using a 5 µm syringe filter to remove all eukaryotic cells. The sample was diluted once more to reach a final dilution of 1:5000. A total of 250 µL of each sample were loaded in duplicate on a 96-well plate, and 2.5 µL of SYBR Green 100× was added to it. The 96-well plate was then wrapped in aluminum foil and placed for 20 min at 37 °C to allow the reaction to occur. A negative control consisting of phosphate-buffered saline only was included.

The total cell count of the mesenteric lymph nodes was analyzed using a BD Accuri C6 flow cytometer (BD Biosciences, Erembodegem, Belgium) as previously performed [3]. The stained bacterial suspensions were excited with a blue laser (488 nm, 20 mW), which was detected in the FL-1 channel (533/30 nm). The run limits were set at 100 µL with Fast Fluidics and the threshold value on FL1-H was set at 1000.

2.6. Paraffin Embedding and Sectioning

The ileum collected for dissection was first placed in 4% paraformaldehyde to begin the fixation of the tissue. Maximum 24 h later, the fixation was interrupted by first rinsing the tissues 3 times in PBS for a duration of 5 min, then placed in 60% ethanol. The samples were stored at 4 °C until paraffin embedding.

The paraffin embedding was started by two washes of 30 min in 100% ethanol, followed by 2 washes of 60 min in 100% ethanol, then 120 min in 100% ethanol. Next, to

remove the residual fat tissues, a first wash of 60 min in 1:1 ethanol/xylene was performed followed by an overnight incubation in 100% xylene. On the next day, 2 washes of 120 min in 100% xylene were performed followed by 2 washes of 120 min each in paraffin. Finally, the paraffin embedding was finalized by placing the tissues in the right orientation in plastic cups, covered in paraffin, and left to harden overnight.

The sectioning of the tissues was made using a Thermo Scientific HM 340E Electronic Rotary Microtome perpendicular to the long axis of the intestine and mounted onto Superfrost^{TM} microscope slides (Thermo Fisher Scientific, Merelbeke, Belgium). Slices of 5 μm paraffin-embedded tissue were realized and stored for further staining.

2.7. Eosin and Hematoxylin Staining

The eosin and hematoxylin staining was performed on the 58 ileum section slides corresponding to the two time points, PID1 and PID7. First, a deparaffination and rehydration step was carried out by performing a 5-min bath of xylene and ethanol 100% twice then a bath of demi-water. Then the hematoxylin staining was performed for 3 min followed by a washing step with tap water for 10 min. The eosin staining was performed for 10 s then the slides were rinsed in demi-water and tap water. A dehydration step was then performed by two baths of 5 min in ethanol 100% followed by 2 baths of 5 min in xylene. The slides were then covered by mounting medium (DEPEX) and a coverslip and dried overnight.

The imaging was performed using a bright-field Nikon Ti-Eclipse microscope (Nikon Belux, Brussels, Belgium) and a 20× objective. The villus length and crypt depth were measured at 10 random places, in 10 sections per mouse, using ImageJ.

2.8. Diaminobenzidine (DAB) Mediated TUNEL Staining

To assess the impact of irradiation in terms of cell death, the terminal deoxynucleotidyl transferase-mediated dUTP nick end labeling (TUNEL) staining was performed using the In Situ Cell Death Detection Kit (#11684817910 Roche, Merck, Aartselaar, Belgium). Briefly, the sections were first deparaffinized and rehydrated, an antigen retrieval step was performed using an antigen retrieval buffer (1/10; DAKO Envision + HRP), three times, 5 min at 600 watts. The endogenous peroxidase activity was then blocked using methanol and 0.3% hydrogen peroxide. The slides were washed with Tris-buffered saline-Triton (TBS-T) (1×, pH 7.6). The TUNEL reaction mixture (1/10) was then added and incubated for 1 h at 37 °C. A signal converter was then added (1/2) and incubated for 30 min at 37 °C. The slides were again washed with PBS, and TRIS (0.5 M, pH 7.4). For visualization, the DAKO Envision+ HRP (Thermo Fisher Scientific, Merelbeke, Belgium) system was used. The slides were placed in 100 mg of 3,3'-diaminobenzidine (DAB) diluted in 0.2 μm filtered TRIS and 33% hydrogen peroxide for 3 min. The reaction with DAB was stopped using TRIS and tap water. Hematoxylin was used as a counter stain, the slides were then rehydrated using two baths of 5 min in ethanol 100% followed by 2 baths of 5 min in xylene. The slides were then covered by mounting medium (DEPEX) and a coverslip and dried overnight.

Slides were imaged using a bright-field Nikon Ti-Eclipse microscope and a 20× objective. First, the total number of cells in the crypt was quantified, then the positively stained cells counted in that crypt were normalized to the latter. Per mouse, 50 random crypts were analyzed.

2.9. Western Blot Analysis of Claudin-5 and Occludin

The snap-frozen ileal samples were first thawed on ice, and 200 μL of ice-cold RIPA buffer (50 mM Tris-HCl (pH 7.4), 150 mM NaCl, 1% Triton X-100, 0.5% sodium deoxycholate, 0.1% sodium dodecyl sulfate) containing 1 mM protease inhibitor and 1 mM phosphatase inhibitor was added to each sample, in addition to a homogenization bead. Cell lysis was performed for 1 min at 25 Hz/sec twice using a Tissue Lyzer (Qiagen, Venlo, The Netherlands), then centrifuged at 14,000× *g*, for 10 min at 4 °C. The supernatant was collected and diluted (1:10), then 25 μL were loaded in duplicates in a 96-wells plate. Protein concentration was measured using a bicinchoninic acid assay (Sigma-Aldrich, Overijse,

Belgium), and 30 μg was loaded on a 1% sodium dodecyl sulfate-polyacrylamide gel, at 100 V for 15 min then 180 V for 45 min. The proteins were then transferred on a nitrocellulose membrane that was first stained with reversible Ponceau S to allow quantification using a Fusion FX imager (Vilber Lourmat, Collégien, France). The Ponceau was then rinsed with PBS-Triton 0.2%, and the membrane was cut at the appropriate height as Claudin 5 and Occludin have different molecular weights. Both were blocked with the blocking buffer (5% non-fat milk; PBS-Triton 0.2%) for 1 h at room temperature, then the primary antibody, anti-Claudin 5 (1:500) (23 kDa, #35-2500, Invitrogen, Waltham, MA, USA) or anti-Occludin were added (1:250) (65 kDa, #40-4700, Invitrogen, Waltham, MA, USA) for incubation overnight at 4 °C. The membranes were rinsed with PBS-Triton 0.2% three times then the secondary antibody was added: anti-mouse goat HPR-linked (3:10,000) (#P0447, DAKO, Agilent, Machelen, Belgium) to bind the anti-claudin 5 primary antibody and the anti-rabbit goat HPR-linked (3:10,000) (#P0447, DAKO, Agilent, Machelen, Belgium) to bind the anti-Occludin primary antibody for 1 h at room temperature. Enhanced chemiluminescence (ECL) was used to assess protein abundance, using a Fusion X imager (Vilber Lourmat, Collégien, France)and ImageJ software 1.53 K Java 13.0.6 (National Institutes of Health, Stapleton, NY, USA).

2.10. Fecal DNA Extraction, DNA Quantification, and 16S rRNA Gene Sequencing

Throughout the supplementation of the PID 7 mice, the fecal pellet was collected longitudinally and snap-frozen in liquid nitrogen until further use. The DNeasy PowerSoil Pro Kit was used to extract total fecal DNA (Qiagen, Venlo, The Netherlands) following the manufacturer's instructions. The extracted DNA was then quantified using the QuantiFluor dsDNA system (Promega, Leiden, The Netherlands).

The high-throughput amplicon sequencing of the V1–V9 hypervariable region was performed at the VIB (Vlaams Instituut voor Biotechnologie, Leuven, Belgium). Briefly, the concentration in gDNA of the samples was first checked with Nanodrop and Qubit, and a PCR was started with 0.5 to 2.5 ng of each sample according to the Pacific BioSciences protocol Amplification of Full-Length 16S Gene with Barcoded Primers for Multiplexed SMRTbell® Library Preparation and Sequencing 101-599-700 Version 04 (January 2021). The SMRTbell was prepared using the SMRTbell Express Template prep kit 2.0, starting with 1034 ng. The bound complex was made using the Polymerase binding kit 2.1. The calculation steps for the Binding, Annealing, and Sequel II run were calculated using SMRT Link: 10.2.0.133434; Chemistry Bundle: 10.2.0.133424; Params: 10.2.0. The sequencing was carried out on a Sequel IIe instrument (PacBio, Menlo Park, CA, USA) on an 8M SMRTcell. The on-plate concentration was 100 pM, using 30 min pre-extension time and 10 h movie time. Positive and negative controls were included according to the manufacturer's recommendations.

2.11. Sequencing Data Processing, Diversity Analysis, and Taxonomic Discovery Analysis

The analysis of the sequencing data was performed by a modified version of SCK CEN developed pipeline entitled OCToPUS pipeline [10], yet activating pacbio option within fasta file extraction, quality filtering, alignment and denoising (mothur, v.1.39.1, [11] using trim.seqs, align.seqs, pre.cluster commands, respectively), chimera-removal (CATCh, v.1.0, [12]) and using UPARSE, the operational taxonomic units (OTUs) were clustered with 97% clustering cut-off. Only a maximum of eight homopolymers and 0 ambiguity were tolerated, and read lengths were trimmed using a window of 60 as an average quality score. The Ribosomal Database Project (RDP) dataset (v.16, [13]) was used for the alignment and classification with an 80% cut-off. The alpha diversity indices were calculated using the Shannon and Chao indices while the beta diversity was estimated through ThetaYC. A non-metric multidimensional scaling (NMDS) was used to visualize the distances. The statistical analysis of the alpha diversity was performed using a linear mixed effects model to account for repeated measures. The beta diversity was analyzed

using the Analysis of Molecular Variance (AMOVA; i.e., ANOVA-like statistical method developed for metagenomic datasets).

The taxonomic discovery analysis was performed using the linear discriminant analysis (LDA) effect size (LEfSe) method [14] using the mothur commands with an LDA cut-off of 3. This method aims to provide biologists with biomarkers capable of explaining the differences observed between two or more conditions. It is performed by first detecting significance using standard tests followed by additional tests asserting biological consistency and effect relevance [14].

The purity of the identified differentially abundant OTUs was further assessed using the oligotyping [15] approach. By splitting some of the OTUs into more than one sub-OTUs, we were able to distinguish up to a single nucleotide. The identified oligotypes were classified with NCBI Nucleotide BLAST using default settings and the RDP database as a reference.

2.12. Statistical Analysis

The statistical analysis was performed on GraphPad Prism Version 9.3.0. (GraphPad Software, San Diego, CA, USA) The outliers were excluded using Tukey's fences criteria, the values below $Q1 - 1.5 \times IQR$ and above $Q3 + 1.5 \times IQR$ were excluded from further statistical analysis. The statistical significance was determined using Kruskal–Wallis, a non-parametric one-way ANOVA test. If significance was found, a multiple-comparison correction was then performed. The differences with a $p < 0.05$ were considered statistically significant, and a tendency was attributed when $0.05 < p < 0.1$.
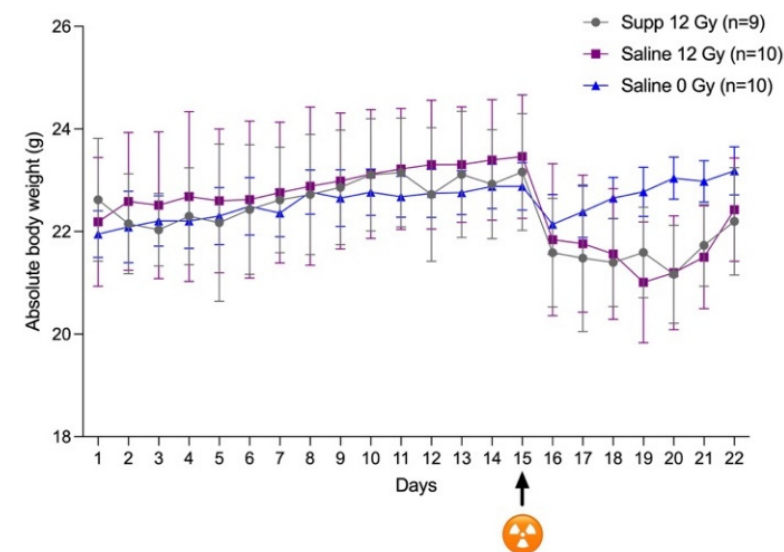
3. Results

3.1. Pelvic Irradiation Induces Changes in Body Weight and Ileal Morphology

To assess the impact of daily supplementation on the mice, the body weight was monitored throughout the duration of the experiment and revealed no significant difference between the three groups before irradiation (Figure 2a). Following the (sham-) irradiation procedure on day 15, a significant drop in the body weight was observed across all groups with a *p*-value of 0.043 for the sham-irradiated group, 0.028 for the saline irradiated group and finally 0.014 for the supplemented irradiated group. The sham-irradiated mice were able to regain weight and recover their original body weight more rapidly than the two irradiated groups regardless of the administered solution.
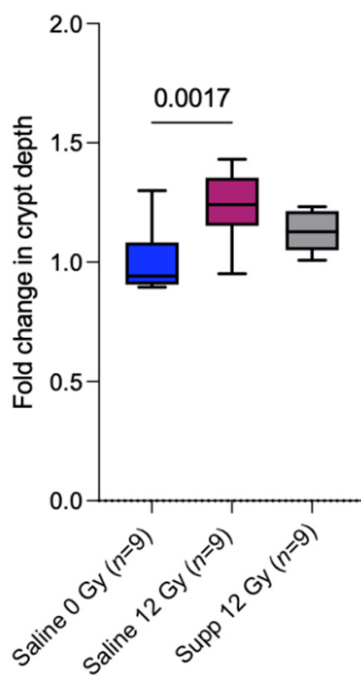
The general morphology of the ileum was closely monitored using immunohistochemistry. The histopathology performed on the ileal sections revealed no significant differences in the crypt depth and villus length at PID1 across the different groups (data not shown). At PID7, a significant increase in crypt depth and villus length was observed between the saline 0 Gy mice and the saline 12 Gy mice, with a *p*-value of 0.0017 and 0.0116, respectively (Figure 2b,c). No significant difference could be detected when comparing the sham-irradiated mice to the supplemented 12 Gy mice allowing us to hypothesize on the ability of the supplementation to prevent or reduce the damages induced by pelvic irradiation.

3.2. The Supplementation Mitigates the Impairment of the Mucosal Barrier Induced by Pelvic Irradiation
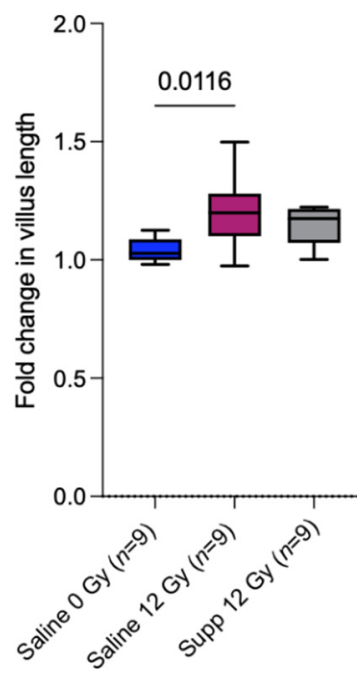
To assess the integrity of the intestinal epithelial layer following pelvic irradiation, ileal thin sections were inspected by microscopy. The direct damage was characterized by a strong increase in the number of apoptotic nuclei present in the intestinal crypts, as soon as one day following irradiation; with an increase of 18% for the saline 12 Gy mice, and 16% for the supplemented 12 Gy mice compared to the sham-irradiated mice (Figure 3a–d). Thus, the supplementation does not appear to protect the intestinal crypts from apoptosis following pelvic irradiation.

(**a**)

(**b**)   (**c**)

Figure 2. Pelvic irradiation induces body weight loss accompanied by morphological changes in the ileal crypts and villus. (**a**) Curve of the absolute body weight of all mice subdivided into three groups throughout the three weeks of supplementation: saline 0 Gy, saline 12 Gy, supplemented 12 Gy. (**b**) Boxplots showing the fold change in ileal crypt depth at PID7 following pelvic (sham-) irradiation for the three groups in respect to a reference sample from the saline 0 Gy group. (**c**) Boxplots showing the fold change in ileal villus length at PID7 following pelvic (sham-) irradiation for the three groups with respect to a reference sample from the saline 0 Gy group. Supp = supplemented, PID = post-irradiation.
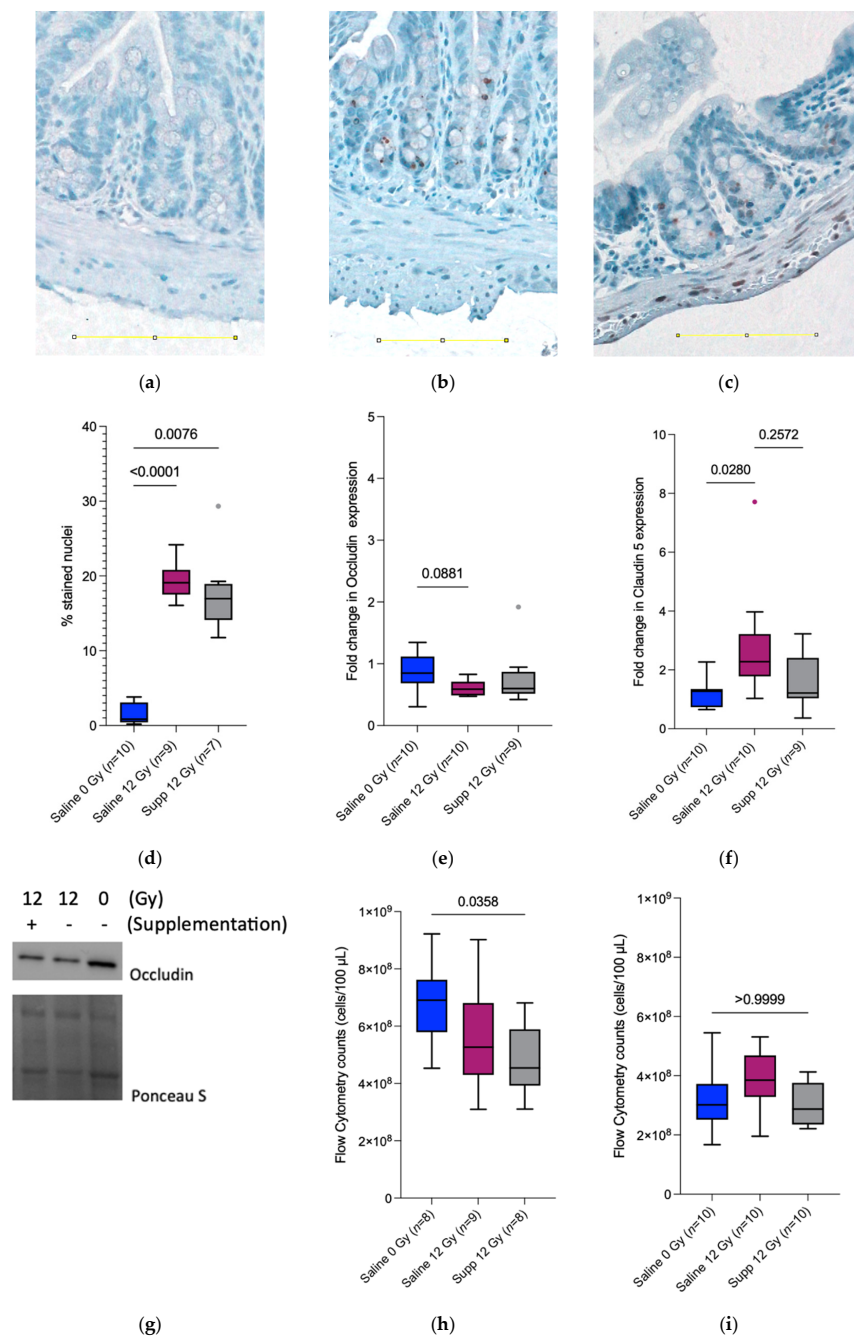
Figure 3. Pelvic irradiation impairs the intestinal epithelial barrier, which is attenuated in the supplemented mice. (**a**–**c**) Representative images of the TUNEL staining obtained for the 3 groups at PID1, the scale bar represents 100 μm for the (**a**) saline 0 Gy group, (**b**) saline 12 Gy group, and (**c**) supplemented 12 Gy group. (**d**) Boxplots representing the ratio of TUNEL + stained nuclei in the crypt to the average number of nuclei forming the said ileal crypts at PID1 following pelvic (sham-)irradiation for the three groups. The data are presented as means ± standard deviation, with $n \geq 9$ per group. Boxplots showing the fold change in (**e**) Occludin and (**f**) Claudin 5 protein expression in the ileum following pelvic (sham-)irradiation at PID7 for the three groups with $n \geq 9$ per group in comparison to a reference sample from the saline sham-irradiated group. (**g**) Representative Western Blot images of Occludin and Ponceau S total protein staining at PID7, $n \geq 8$ per group. Bacterial counts obtained by flow cytometry performed on the mesenteric lymph nodes following pelvic (sham-)irradiation at (**h**) PID1 and (**i**) PID7 for the three groups: saline 0 Gy, saline 12 Gy, supplemented 12 Gy with $n \geq 8$ per group. Supp = supplemented, PID = post-irradiation day.

Next, the expression of two tight junction proteins, Occludin and Claudin 5 was assessed. One day following irradiation, no significant difference in the protein expression of either tight junction protein was detected across the different groups (Figure S1a,b). One week following irradiation, a decreasing tendency was detected in the Occludin protein expression in the saline 12 Gy mice compared to the sham-irradiated mice, with a *p*-value of 0.0881 (Figure 3e). Interestingly, the Occludin protein was not found differentially expressed between the supplemented irradiated mice and the sham-irradiated mice. Surprisingly, the expression of the Claudin 5 protein at PID7 increased in the saline irradiated group compared to the saline sham-irradiated group whereas no differential expression was detected between the saline sham-irradiated group and the supplemented irradiated group (Figure 3f).

To further correlate with these observations, the potential bacterial translocation towards the mesenteric lymph nodes was measured using flow cytometry. One day following (sham-) irradiation, a significant decrease in the bacterial count was observed between the irradiated mice receiving the supplementation and the sham-irradiated mice with a *p*-value of 0.0358 (Figure 3h). Interestingly, seven days following (sham-) irradiation, no significant difference was observed between the two groups above-mentioned (Figure 3i). Thus, the supplementation seems to confer tight junction protection seven days following 12 Gy pelvic irradiation.

3.3. The Shift in the Microbial Population Induced by Pelvic Irradiation Is Prevented by Supplementation

The impact of supplementation and irradiation on the gut microbiota was analyzed using 16S rRNA gene sequencing. The PID0 (i.e., before irradiation), PID1, and PID7 time points were specifically analyzed. To first ensure that the sequencing procedure was able to capture most of the diversity in the samples, the gene richness and Good's estimator of coverage were looked at. The phase plateau was reached allowing a conclusion to be drawn on the adequate level of sequencing (Figure 4a). The average estimated coverage was greater than 99.9% and confirmed the sequencing depth (Figure 4b). A total of 4448 OTUs were found among the samples, with around 300 OTUs showing a relative abundance above 0.1%.

To assess the impact of supplementation on the composition of the microbiota, alpha diversity (diversity within a sample) and beta diversity (diversity between the samples) were analyzed across the groups at different time points, therefore excluding the variation introduced by the different studied parameters. In saline irradiated (Figure 4d) and, to a lesser extent, in saline sham-irradiated (Figure 4c) mice, a transient increase in alpha diversity is apparent at PID1 as measured by the Shannon index (considering microbial richness and the evenness). In supplemented irradiated mice, this increase in alpha diversity lasted longer, remaining significant even at PID7 (Figure 4e).

Next, the beta diversity was analyzed using the distance matrix ThetaYC, accounting for the relative abundances. The saline sham-irradiated group did not experience any shift in beta diversity throughout the different time points (Figure 4f). When looking at the saline irradiated mice exclusively, a significant shift in the beta diversity was observed at PID7 compared to PID0 with a *p*-value of 0.048 (Figure 4g). Interestingly, when looking at the supplemented irradiated group, no significant shift in the beta diversity could be detected when compared to PID0 (Figure 4h).
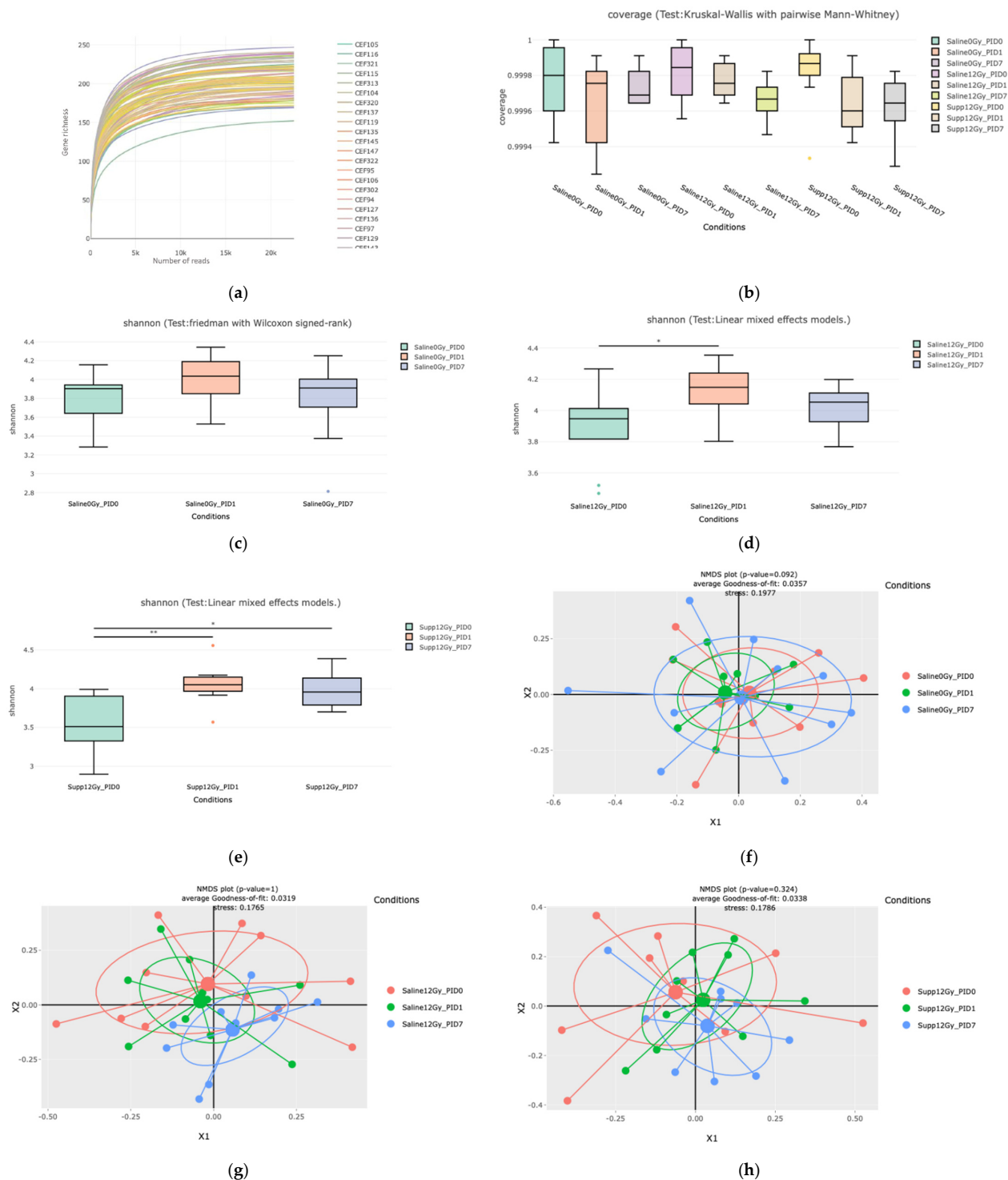
(**a**)

(**b**)

(**c**)

(**d**)

(**e**)

(**f**)

(**g**)

(**h**)

Figure 4. Pelvic irradiation induces a shift in beta diversity that is prevented by supplementation. (**a**) Good's estimator of coverage: rarefaction curve showing the gene richness in the function of the number of reads per sample. (**b**) Boxplots showing the coverage obtained by the sequencing for the three different groups analyzed at the three different time points. Shannon index measuring the alpha diversity, considering the richness and the evenness of the samples at PID0, PID1, and PID7 for (**c**) the saline 0 Gy group, for (**d**) the saline 12 Gy group, and the (**e**) supplemented 12 Gy group, with $n = 9$. ** $p < 0.01$, * $p < 0.05$. (**f**) ThetaYC non-metric multidimensional scaling distance matrix measuring the beta diversity among the saline 0 Gy group, (**g**) the saline 12 Gy, and (**h**) among the supplemented 12 Gy group, with $n \geq 9$ per group. PID = post-irradiation day.

To further analyze the microbial communities following pelvic irradiation and address the impact of supplementation in mitigating the effect of irradiation, we used the LEfSe method. We focused on the different cohorts and analyzed the evolution in relative abundance in the members of their microbial community compared to their baseline community at PID0. For the saline sham-irradiated group, we were able to detect 6 OTUs that were more abundant compared to the baseline throughout the experiment belonging to the *Muribaculaceae, Prevotellaceae, Butyricicoccaceae,* and *Ruminococcaceae* families, indicating a relatively stable community over time (Table 1). Furthermore, the saline irradiated group presented an increased number of differentially abundant OTUs, mainly belonging to the *Lachnospiraceae* and *Bacteroidaceae* families (Table 2). Finally, the supplemented group demonstrated the most important shift in OTU abundance. Specifically, 6 OTUs belonging to the *Lachnospiraceae* family were found to be more enriched at PID1 whereas 2 OTUs belonging to the *Ruminococcaceae* family were more abundant at PID7. Interestingly, an OTU belonging to the cyanobacteria phylum was more abundantly detected at PID7 (Table 3). The NCBI Nucleotide BLAST was able to provide a hit corresponding to the OTU_178 belonging to the *Rikinellaceae* family, being *Alistipes putredinis.* It is, in addition, important to mention that both irradiated groups demonstrated an increasing abundance at PID7 in OUT_44 and OTU_77 belonging to the *Ruminococcaceae* and *Clostridiaceae* families, respectively.

Table 1. Differentially abundant OTUs among the saline sham-irradiated group at PID1 and PID7 compared to the baseline at PID0. RDP = Ribosomal Database Project.

Timepoint	Taxonomic Classification (Family) (Following the RDP Database)	Highest NCBI Blast Hit (% Identity)
PID 1	*Muribaculaceae* OTU_45 *Prevotellaceae* OTU_12 *Rhodospirillales* OTU_87 (order)	
PID 7	*Muribaculaceae* OTU_75 *Butyricicoccaceae* OTU_123 *Ruminococcaceae* OTU_127	

Table 2. Differentially abundant OTUs among the saline irradiated group at PID1 and PID7 compared to the baseline at PID0. RDP = Ribosomal Database Project.

Timepoint	Taxonomic Classification (Family) (Following RDP Database)	Highest NCBI Blast Hit (% Identity)
PID 1	*Butyricicoccaceae* OTU_123 *Lachnospiraceae* OTU_183 *Lachnospiraceae* OTU_93 *Ruminococcaceae* OTU_44	*Limosilactobacillus reuteri* (99.8%)
PID 7	*Muribaculaceae* OTU_75 *Bacteroidaceae* OTU_98 *Bacteroidaceae* OTU_134 *Clostridiaceae* OTU_77 *Lachnospiraceae* OTU_133	*Bacteroides caecimuris* (100%) *Bacteroides acidifaciens* (99.79%)

Table 3. Differentially abundant OTUs among the supplemented irradiated group at PID1 and PID7 compared to the baseline at PID0. RDP = Ribosomal Database Project.

Timepoint	Taxonomic Classification (Family) (Following the RDP Database)	Highest NCBI Blast Hit (% Identity)
PID 1	*Prevotellaceae* OTU_12	
	Lachnospiraceae OTU_42	
	Lachnospiraceae OTU_15	
	Lachnospiraceae OTU_4	
	Lachnospiraceae OTU_126	
	Lachnospiraceae OTU_159	
	Lachnospiraceae OTU_128	
	Ruminococcaceae OTU_44	
	Gastranaerophilales OTU_97	
PID 7	*Clostridiaceae* OTU_77	
	Rikenellaceae OTU_178	*Alistipes putredinis* (97.03%)
	Ruminococcaceae OTU_127	

4. Discussion

Radiotherapy-related complications have been reported since the first applications in humans and remain the primary reason for treatment delay or interruption. In this set of experiments, and in continuity with the previous work performed [7], we investigated the combination of both *L. indica* PCC 8005 and *L. rhamnosus* GG supplementation for their ability to mitigate the mucositis and dysbiosis induced in a mouse model following pelvic irradiation.

We hypothesized that by combining these bacterial food supplements, their individual beneficial effects may be additive or synergistic. Indeed, *Spirulina* was previously investigated in vitro with various *Lactobacillus* strains. The mixture of *Spirulina* with several lactic acid species (*Lactiplantibacillus plantarum, Lacticaseibacillus casei,* and *Lactobacillus acidophilus*) improved the protein content, the amino acid content as well as the antibacterial activity exhibited by the cyanobacteria [16]. Furthermore, the growth of lactic acid bacteria such as *L. casei* and *L. acidophilus* in the presence of dry biomass of *Arthrospira platensis* was enhanced [17].

First, we were able to confirm that anesthesia followed by (sham-) irradiation temporally impacts the total body weight of the mice as observed by Segers et al. [3]. It is explained by the decreased food and water intake following anesthesia and (sham-) irradiation that in turn might be explained by the lowered locomotor activity that was recorded by Wolff et al. when investigating the fatigue-like behavior experienced by mice following pelvic irradiation [18]. We found that the combined administration of *L. indica* PCC 8005 and *L. rhamnosus* GG at the same dosage as when delivered individually, did not prevent nor speed up restoration of body weight following anesthesia and 12 Gy pelvic irradiation. This is in contradiction with the diminished weight loss and the faster regain observed by Ciorba et al. when mice were treated with 5×10^7 *L. rhamnosus* GG uniquely for three days by oral gavage, before 12 Gy whole-body irradiation [19]. This difference could be explained by the more drastic systemic failure induced by whole-body irradiation compared to the more subtle effects caused by localized pelvic irradiation.

Second, the disruption of the mucosal homeostasis caused by 12 Gy pelvic irradiation was translated by a significant increase in the crypt depth and villus length, 7 days following pelvic irradiation with only an increasing tendency in villus length for the supplemented irradiated group. In the crypts reside the stem cells that allow the constant renewal of the intestinal epithelial layer as those cells differentiate and migrate along the intestinal villi and are therefore highly sensitive to irradiation. Fortunately, due to the compensatory proliferation of the stem cells and the low irradiation dose applied, a post-irradiation regeneration is observed among the crypts and the villus [20]. Accordingly, the increase in apoptotic nuclei further correlates with the high sensitivity characterizing the stem cells located in the intestinal crypts. We can speculate that the absence of differences

between the supplemented group and the control group with respect to the crypt and villus shortening could be explained by the ability of *L. rhamnosus* GG to activate the anti-apoptotic Akt/Protein kinase B pathway and inhibit the pro-apoptotic p38/mitogen-activated protein kinase [21].

We then investigated the intestinal barrier integrity, which is known to be impaired by radiotherapy [3,22]. At PID1, the significant decrease observed in bacterial translocation towards the mesenteric lymph nodes in the supplemented irradiated mice could be explained by the microbicidal activity of the infiltrating neutrophils [23]. In addition, *L. rhamnosus* GG and *L. indica* PCC 8005 were found to produce different types of antimicrobial compounds efficient against Gram-negative and Gram-positive bacteria [24]. Similarly, *L. rhamnosus* GG was found to produce seven peptides exhibiting antibacterial effects against Gram-negative and Gram-positive bacteria [25]. This decrease in the total bacterial count in the mesenteric lymph nodes observed at PID1 is absent at PID7. This can be explained by the ability of *L. rhamnosus* GG and *L. indica* PCC 8005 to protect the intestinal barrier that has been investigated for *L. plantarum* and which was found to protect rats from *E. coli*-induced increased intestinal permeability following one week of pretreatment with 10^9 CFU [26]. Similarly, the administration of 10^8 CFU of *L. rhamnosus* GG once a day for 13 days to a chemotherapy-induced mucositis Balb/c mice model, was found to attenuate weight loss and intestinal permeability by increasing the production of intestinal mucus [27].

To further assess the integrity of the intestinal barrier and correlate with the bacterial counts in the mesenteric lymph nodes, the status of two tight junction proteins was monitored. Claudin 5 is a transmembrane protein present in the tight junctions of endothelium and epithelium barriers, regulating paracellular ionic selectivity. It is found to be colocalized with Occludin, another transmembrane protein associated with cytoskeletal signaling proteins. Surprisingly, and in contradiction with previous results [3,28], the claudin 5 protein expression increased 1 week following irradiation for the saline 12 Gy group while the expression remained the same when comparing the supplemented irradiated group to the saline sham-irradiated group, indicating the potential ability of the supplementation to counteract the radiation-induced side effects. Furthermore, the Occludin expression remained unchanged between the irradiated group receiving the supplements and the sham-irradiated group receiving saline 7 days following (sham-) irradiation. The ability of *L. plantarum*, MB452 a probiotic strain was investigated for its capacity to enhance the intestinal barrier function and was found to promote the expression of proteins involved in the signaling occurring at the tight junction level [29,30]. In contrast, this ability was investigated for *L. rhamnosus* GG and *L. indica* PCC 8005 independently [8]; the tested supplements failed to intervene and protect the epithelial barrier at the level of the tight junction proteins.

Following 16S metagenetic analysis, we were able to detect an increase in richness and evenness in the supplemented group, sustained through time in comparison to the irradiated group where this shift was only shown to be transient. This increase was previously reported [7], at PID3 following 12 Gy pelvic irradiation, when 7×10^8 cells/mouse of *L. rhamnosus* GG were administered to mice. Similarly, Zhao et al. were able to observe an increase in alpha diversity following 14 days of supplementation with a mixture of lactobacilli (including *L. rhamnosus*) before a 9 Gy total body irradiation [31]. On the other hand, Li et al. directed their study toward the active principle found in *Limnospira* sp. i.e., phycocyanin. They were able to show that the administration of this compound in pretreatment or in a therapeutic manner was able to increase the alpha diversity of the intestinal microbiota following a 20 Gy thoracic irradiation [32].

When looking at the beta diversity, we can exclude any effect of oral gavage as the saline sham-irradiated group did not present any changes in the microbial composition through the different time points. The beta diversity among the supplemented irradiated group demonstrated the efficacy of the combinatorial bacterial food supplementation as no dysbiotic state was detected throughout the different time points studied. This observation was further validated by the shift observed among the saline irradiated group

when comparing PID0 to PID7. Therefore, the dysbiosis was prevented or corrected by the administration of the bacterial food supplement. This shift in the beta diversity seven days following irradiation was similarly observed in our previous study, for the mice supplemented with *L. rhamnosus* GG only but not with *L. indica* PCC 8005 [7]. Zhao et al. also observed a shift in beta diversity following the administration of a mixture of lactobacilli species before a 9 Gy total body irradiation [31]. To our knowledge, this is the first report investigating the alpha and beta diversity changes following the combined administration of *L. rhamnosus* GG and *L. indica* PCC 8005 to mice.

In continuity with the analysis of the beta diversity, the most differentially abundant OTUs present in the cohorts at the studied time points revealed interesting observations. The enriched presence in *Lachnospiraceae*, *Ruminococcaceae*, and *Clostridiaceae* members in both irradiated groups was previously reported [3], and also observed by Goudarzi et al. [33] in mice exposed to 12 Gy pelvic and total body irradiation, respectively. Interestingly, the *Lachnospiraceae* members have been found to attenuate the gastrointestinal damages induced by a 9 Gy total body irradiation in a mice model [34], which may support the important increase observed in *Lachnospiraceae* members in the supplemented group supporting our previous findings. As similarly observed by Segers et al. [7], the increased abundance of *Alistipes putredinis* associated with the supplemented group at PID7 may correlate with the intervention of this genus in a harmful or beneficial manner on multiple scenes including dysbiosis, colorectal cancer, colitis, and cardiovascular diseases [35,36]. Moreover, the identification of *Bacteroides acidifaciens* further confirms the dysbiotic state induced by irradiation as it was found to be increased in the context of inflammation [37].

The beneficial effects demonstrated above pave the way for further research on both compounds as their complementary administration enhances their protective nature towards irradiation-induced dysbiosis and prevents the increase in villus length and crypt depth, whereas individual administration of the same compounds was only able to prevent irradiation-induced dysbiosis. Further research using in vitro assays including human gut organoids-derived bioreactor may further demonstrate the molecular interactions occurring at the level of the different strains in response to the administration of *L. rhamnosus* GG and *L. indica* PCC 8005 where the administered dose is no longer limited by the oral gavage capacity.

References

1. Yeung, C.-Y.; Chan, W.-T.; Jiang, C.-B.; Cheng, M.-L.; Liu, C.-Y.; Chang, S.-W.; Chiau, J.-S.C.; Lee, H.-C. Amelioration of chemotherapy-induced intestinal mucositis by orally administered probiotics in a mouse model. *PLoS ONE* **2015**, *10*, e0138746. [CrossRef]
2. Keefe, D.M.K.; Gibson, R.J.; Hauer-Jensen, M. OBJECTIVE: To review the management of ra-diotherapy-and chemotherapy-induced gastrointestinal mucositis. *Gastrointest. Mucositis* **2004**, *20*, 38–47. [CrossRef]
3. Segers, C.; Mysara, M.; Claesen, J.; Baatout, S.; Leys, N.; Lebeer, S.; Verslegers, M.; Mastroleo, F. Intestinal mucositis precedes dysbiosis in a mouse model for pelvic irradiation. *ISME Commun.* **2021**, *1*, 24. [CrossRef]
4. Motiani, K.K.; Collado, M.C.; Eskelinen, J.J.; Virtanen, K.A.; Löyttyniemi, E.; Salminen, S.; Nuutila, P.; Kalliokoski, K.K.; Hannukainen, J.C. Exercise training modulates gut microbiota profile and improves endotoxemia. *Med. Sci. Sports Exerc.* **2020**, *52*, 94–104. [CrossRef] [PubMed]
5. Shi, C.-W.; Cheng, M.-Y.; Yang, X.; Lu, Y.-Y.; Yin, H.-D.; Zeng, Y.; Wang, R.-Y.; Jiang, Y.-L.; Yang, W.-T.; Wang, J.-Z.; et al. Probiotic *Lactobacillus rhamnosus* GG Promotes Mouse Gut Microbiota Diversity and T Cell Differentiation. *Front. Microbiol.* **2020**, *11*, 607735. [CrossRef]
6. Badri, H.; Monsieurs, P.; Coninx, I.; Wattiez, R.; Leys, N. Molecular investigation of the radiation resistance of edible cyanobacterium *Arthrospira* sp. PCC 8005. *Microbiologyopen* **2015**, *4*, 187–207. [CrossRef]
7. Segers, C.; Mysara, M.; Coolkens, A.; Wouters, S.; Baatout, S.; Leys, N.; Lebeer, S.; Verslegers, M.; Mastroleo, F. *Limnospira indica* PCC 8005 Supplementation Prevents Pelvic Irradiation-Induced Dysbiosis but Not Acute Inflammation in Mice. *Antioxidants* **2023**, *12*, 572. [CrossRef]
8. Segers, C.; Mysara, M.; Coolkens, A.; Baatout, S.; Leys, N.; Lebeer, S.; Verslegers, M.; Mastroleo, F. *Limnospira indica* PCC 8005 or *Lacticaseibacillus rhamnosus* GG Dietary Supplementation Modulate the Gut Microbiome in Mice. *Appl. Microbiol.* **2022**, *2*, 636–650. [CrossRef]
9. Cogne, G.; Lehmann, B.; Dussap, C.G.; Gros, J.B. Uptake of macrominerals and trace elements by the cyanobacterium Spirulina platensis (*Arthrospira platensis* PCC 8005) under photoautotrophic conditions: Culture medium optimization. *Biotechnol. Bioeng.* **2003**, *81*, 588–593. [CrossRef]
10. Mysara, M.; Njima, M.; Leys, N.; Raes, J.; Monsieurs, P. From reads to operational taxonomic units: An ensemble processing pipeline for MiSeq amplicon sequencing data. *GigaScience* **2017**, *6*, giw017. [CrossRef]
11. Schloss, P.D.; Westcott, S.L.; Ryabin, T.; Hall, J.R.; Hartmann, M.; Hollister, E.B.; Lesniewski, R.A.; Oakley, B.B.; Parks, D.H.; Robinson, C.J.; et al. Introducing mothur: Open-source, platform-independent, community-supported software for describing and comparing microbial communities. *Appl. Environ. Microbiol.* **2009**, *75*, 7537–7541. [CrossRef] [PubMed]
12. Mysara, M.; Saeys, Y.; Leys, N.; Raes, J.; Monsieurs, P. CATCh, an ensemble classifier for chimera detection in 16s rRNA sequencing studies. *Appl. Environ. Microbiol.* **2015**, *81*, 1573–1584. [CrossRef]
13. Wang, Q.; Garrity, G.M.; Tiedje, J.M.; Cole, J.R. Naïve Bayesian classifier for rapid assignment of rRNA sequences into the new bacterial taxonomy. *Appl. Environ. Microbiol.* **2007**, *73*, 5261–5267. [CrossRef] [PubMed]
14. Segata, N.; Izard, J.; Waldron, L.; Gevers, D.; Miropolsky, L.; Garrett, W.S.; Huttenhower, C. Metagenomic biomarker discovery and explanation. *Genome Biol.* **2011**, *12*, R60. [CrossRef]
15. Berg, G.; Rybakova, D.; Fischer, D.; Cernava, T.; Vergès, M.-C.C.; Charles, T.; Chen, X.; Cocolin, L.; Eversole, K.; Corral, G.H.; et al. Microbiome definition re-visited: Old concepts and new challenges. *Microbiome* **2020**, *8*, 103. [CrossRef]
16. Yu, J.; Ma, D.; Qu, S.; Liu, Y.; Xia, H.; Bian, F.; Zhang, Y.; Huang, C.; Wu, R.; Wu, J.; et al. Effects of different probiotic combinations on the components and bioactivity of Spirulina. *J. Basic Microbiol.* **2020**, *60*, 543–557. [CrossRef]
17. Bhowmik, D.; Dubey, J.; Mehra, S. Probiotic Efficiency of Spirulina platensis-Stimulating Growth of Lactic Acid Bacteria. *World J. Dairy Food Sci.* **2009**, *4*, 160–163.
18. Wolff, B.S.; Raheem, S.A.; Alshawi, S.A.; Regan, J.M.; Feng, L.R.; Saligan, L.N. Induction of fatigue-like behavior by pelvic irradiation of male mice alters cognitive behaviors and BDNF expression. *PLoS ONE* **2020**, *15*, e0235566. [CrossRef]
19. Ciorba, M.A.; Riehl, T.E.; Rao, M.S.; Moon, C.; Ee, X.; Nava, G.; Walker, M.R.; Marinshaw, J.M.; Stappenbeck, T.S.; Stenson, W.F. Lactobacillus probiotic protects intestinal epithelium from radiation injury in a TLR-2/cyclo-oxygenase-2-dependent manner. *Gut* **2012**, *61*, 829–838. [CrossRef]
20. Tian, H.; Biehs, B.; Warming, S.; Leong, K.G.; Rangell, L.; Klein, O.D.; De Sauvage, F.J. A reserve stem cell population in small intestine renders Lgr5-positive cells dispensable. *Nature* **2011**, *478*, 255–259. [CrossRef] [PubMed]
21. Yan, F.; Polk, D.B. Probiotic bacterium prevents cytokine-induced apoptosis in intestinal epithelial cells. *J. Biol. Chem.* **2002**, *277*, 50959–50965. [CrossRef]

22. Qu, W.; Zhang, L.; Ao, J. Radiotherapy Induces Intestinal Barrier Dysfunction by Inhibiting Autophagy. *ACS Omega* **2020**, *5*, 12955–12963. [CrossRef]

23. Molloy, M.J.; Grainger, J.R.; Bouladoux, N.; Hand, T.W.; Koo, L.Y.; Naik, S.; Quinones, M.; Dzutsev, A.K.; Gao, J.-L.; Trinchieri, G.; et al. Intraluminal containment of commensal outgrowth in the gut during infection-induced dysbiosis. *Cell Host Microbe* **2013**, *14*, 318–328. [CrossRef] [PubMed]

24. El-Sheekh, M.M.; Daboor, S.M.; Swelim, M.A.; Mohamed, S. Production and Characterization of Antimicrobial Active Substance from Spirulina platensis. Available online: http://ijm.tums.ac.ir (accessed on 5 October 2022).

25. Lu, R.; Fasano, S.; Madayiputhiya, N.; Morin, N.P.; Nataro, J.; Fasano, A. Isolation, Identification, and Characterization of Small Bioactive Peptides from Lactobacillus GG Conditional Media That Exert Both Anti-Gram-negative and Gram-Positive Bactericidal Activity. 2009. Available online: http://journals.lww.com/jpgn (accessed on 5 October 2022).

26. Mangell, P.; Nejdfors, P.; Wang, M.; Ahrné, S.; Weström, B.; Thorlacius, H.; Jeppsson, B. *Lactobacillus plantarum* 299v Inhibits *Escherichia coli*-Induced Intestinal Permeability. *Dig. Dis. Sci.* **2002**, *47*, 511–516. [CrossRef] [PubMed]

27. Trindade, L.M.; Torres, L.; Matos, I.D.; Miranda, V.C.; de Jesus, L.C.L.; Cavalcante, G.; Oliveira, J.J.d.S.; Cassali, G.D.; Mancha-Agresti, P.; Azevedo, V.A.D.C.; et al. Paraprobiotic *Lacticaseibacillus rhamnosus* Protects Intestinal Damage in an Experimental Murine Model of Mucositis. *Probiotics Antimicrob Proteins* **2021**, *15*, 338–350. [CrossRef]

28. Sándor, N.; Walter, F.R.; Bocsik, A.; Sántha, P.; Schilling-Tóth, B.; Léner, V.; Varga, Z.; Kahán, Z.; Deli, M.; Sáfrány, G.; et al. Low dose cranial irradiation-induced cerebrovascular damage is reversible in mice. *PLoS ONE* **2014**, *9*, e112397. [CrossRef]

29. Anderson, R.C.; Cookson, A.L.; McNabb, W.C.; Park, Z.; McCann, M.J.; Kelly, W.J.; Roy, N.C. *Lactobacillus plantarum* MB452 enhances the function of the intestinal barrier by increasing the expression levels of genes involved in tight junction formation. *BMC Microbiol.* **2010**, *10*, 316. [CrossRef] [PubMed]

30. Segers, M.E.; Lebeer, S. Towards a better understanding of *Lactobacillus rhamnosus* GG—Host interactions. *Microb. Cell Fact.* **2014**, *13*, S7. [CrossRef] [PubMed]

31. Zhao, T.-S.; Xie, L.-W.; Cai, S.; Xu, J.-Y.; Zhou, H.; Tang, L.-F.; Yang, C.; Fang, S.; Li, M.; Tian, Y. Dysbiosis of Gut Microbiota Is Associated with the Progression of Radiation-Induced Intestinal Injury and Is Alleviated by Oral Compound Probiotics in Mouse Model. *Front. Cell Infect. Microbiol.* **2021**, *11*, 717636. [CrossRef]

32. Li, W.; Lu, L.; Liu, B.; Qin, S. Effects of phycocyanin on pulmonary and gut microbiota in a radiation-induced pulmonary fibrosis model. *Biomed. Pharmacother.* **2020**, *132*, 110826. [CrossRef]

33. Goudarzi, M.; Mak, T.D.; Jacobs, J.P.; Moon, B.H.; Strawn, S.J.; Braun, J.; Brenner, D.J.; Fornace, A.J., Jr.; Li, H.H. An Integrated Multi-Omic Approach to Assess Radiation Injury on the Host-Microbiome Axis. *Radiat. Res.* **2016**, *186*, 219–234. [CrossRef]

34. Guo, H.; Chou, W.-C.; Lai, Y.; Liang, K.; Tam, J.W.; Brickey, W.J.; Chen, L.; Montgomery, N.D.; Li, X.; Bohannon, L.M.; et al. Multi-omics analyses of radiation survivors identify radioprotective microbes and metabolites. *Science* **2020**, *370*, eaay9097. [CrossRef]

35. Parker, B.J.; Wearsch, P.A.; Veloo, A.C.M.; Rodriguez-Palacios, A. The Genus Alistipes: Gut Bacteria With Emerging Implications to Inflammation, Cancer, and Mental Health. *Front. Immunol.* **2020**, *11*, 906. [CrossRef] [PubMed]

36. Moschen, A.R.; Gerner, R.R.; Wang, J.; Klepsch, V.; Adolph, T.E.; Reider, S.J.; Hackl, H.; Pfister, A.; Schilling, J.; Moser, P.L.; et al. Lipocalin 2 Protects from Inflammation and Tumorigenesis Associated with Gut Microbiota Alterations. *Cell Host Microbe* **2016**, *19*, 455–469. [CrossRef] [PubMed]

37. Panebianco, C.; Potenza, A.; Andriulli, A.; Pazienza, V. Exploring the microbiota to better understand gastrointestinal cancers physiology. *Clin. Chem. Lab. Med.* **2018**, *56*, 1400–1412. [CrossRef] [PubMed]